RECORD QUANTUM EFFICIENCY FROM SUPERLATTICE PHOTOCATHODE FOR SPIN POLARIZED ELECTRON BEAM PRODUCTION *

J.P. Biswas, L. Cultrera, W. Liu, E. Wang, J. Skaritka, K. Kisslinger, Brookhaven National Laboratory
S.D. Hawkins, S.R. Lee, J.F. Klem, Sandia National Laboratories,

Abstract

Electron sources producing highly spin-polarized electron beams are currently possible only with photocathodes based on GaAs and other III-V semiconductors. GaAs/GaAsP superlattice (SL) photocathodes with a distributed Bragg reflector (DBR) represent the state of the art for the production of spin polarized electrons. We present results on a SL-DBR GaAs/GaAsP structure designed to leverage strain compensation to achieve simultaneously high QE and spin polarization. These photocathode structures were grown using molecular beam epitaxy and achieved quantum efficiencies exceeding 15% and electron spin polarization of about 75% when illuminated with near bandgap photon energies.

INTRODUCTION

Polarized electron sources are used in fundamental research in many fields including condensed matter physics and elementary particle physics. Polarized electron sources are employed in polarized electron microscope [1] to study domain walls in ferromagnetic materials. Polarized positron beams can be generated by impinging polarized electron beams in high Z-target elements. The planned International Linear Collider is designed to collide spin-polarized electrons and positrons at large energies in the TeV range. The Electron Ion Collider [2] that will be operated in the USA also requires a spin-polarized electron source for nuclear physics study. Most facilities require a few hundred micro amperes of current that can be easily produced by the current state-of-the-art electron sources [3]. Other facilities such as the Large Hadron electron Collider plans to operate at a high average current of 20 mA, which is beyond the current state of the art.

Spin-polarized electron sources are generated from GaAs based photocathodes. Bulk GaAs with traditional Cs-O activation provides a high QE of around 10%, however, the maximum polarization is limited to 50% due to the degeneracy of the heavy-hole and light-hole at the $2p_{3/2}$ band state. Growing the photocathode strained eliminates the degeneracy thus maximizing the spin polarization. In the 1990s strained GaAs grown on GaAsP showed improved electron spin polarization (ESP) of 75-80%, whereas QE was limited to only about 0.3% [4]. Through the use of strained superlattices (SL) based on GaAs/GaAsP, it was possible to leverage quantum well structures to increase the separation between

heavy and light hole bands and achieve even higher spin polarization (up to 85%) and QE (just above 1%) [5]. Advanced SL-based GaAs photocathodes consist of alternating layers with tensile and compressive strain thus effectively reducing the defect density due to the strain on the SL layer. By reducing defect density, spin polarization could be further increased up to 92% with a QE of just 1.6% [5]. Simultaneously achieving high QE and spin polarization is difficult. As the QE increase due to the larger thickness of the SL layer, spin polarization decreases due to the depolarization mechanism of the electron with the thick layer.

CATHODE WITH DISTRIBUTED BRAGG REFLECTOR

A distributed Bragg reflector (DBR) grown underneath the SL with a buffer medium layer creates a Fabry Perot resonator that effectively traps the light and enhances the QE [6, 7]. Instead of laser light passing through the cathode, it reflects repeatedly within the cavity, increasing photon absorption, which in turn, improves the QE. Such a structure demonstrated record performance achieving ESP of 84% and QE of 6.4% at 776 nm laser wavelength [6]. As the number of layers increases the growth of such structure with high QE and ESP becomes increasingly challenging.

The structural element of the photocathode used in this work is illustrated in Fig. 1. The DBR consists of alternating layer of high (n_H) and low (n_L) index of refraction material. The high refractive index layer is $GaAs_{0.81}P_{0.19}$ and low refractive index layer is $AlAs_{0.78}P_{0.22}$. For a high reflectivity at a certain wavelength lambda, the thickness of the DBR layers are, $\lambda_B/4n_H$, and $\lambda_B/4n_L$ respectively [8]. The bandwidth over which the DBR has high reflectivity can be expressed as [8],

$$\Delta\lambda_B = \frac{4\lambda_B}{\pi} sin^{-1}\left(\frac{n_H - n_L}{n_H + n_L}\right) \qquad (1)$$

The DBR layer consists of 10 pairs of $GaAs_{0.81}P_{0.19}$, and $AlAs_{0.78}P_{0.22}$ with refractive index $n_H = 3.554$, and $n_L = 2.992$ respectively. Thickness are estimated to be around $d_H = 65nm$ and $d_L = 55nm$ respectively. A 300 nm base layer was used to provide the strain compensating lattice constant for the growth of the SL structure and the optical thickness for the tuning of the Fabry-Perot resonator. The strain compensated (-0.7%/+0.7%) SL structure consists of 30 pairs of p-type ($5 \times 10^{17}/cm^3$) $GaAs_{0.62}P_{0.38}/GaAs$ (4/4 nm thickness). The structure is terminated with a 5 nm highly p-doped ($5 \times 10^{19}/cm^3$) GaAs.

GaAs	5 nm	$p = 5\times10^{19}$ cm^{-3}	
GaAs$_{0.62}$P$_{0.38}$	4 nm	$p = 5\times10^{17}$ cm^{-3}	30 pairs
GaAs	4 nm	$p = 5\times10^{17}$ cm^{-3}	
GaAs$_{0.81}$P$_{0.19}$	300 nm	$p = 5\times10^{18}$ cm^{-3}	
AlAs$_{0.78}$P$_{0.22}$	65 nm	$p = 5\times10^{18}$ cm^{-3}	10 pairs
GaAs$_{0.81}$P$_{0.19}$	55 nm	$p = 5\times10^{18}$ cm^{-3}	
GaAs$_{0.81}$P$_{0.19}$	2000 nm	$p = 5\times10^{18}$ cm^{-3}	
GaAs->GaAs$_{0.81}$P$_{0.19}$	2750 nm	$p = 5\times10^{18}$ cm^{-3}	
GaAs buffer	200 nm	$p = 5\times10^{18}$ cm^{-3}	
GaAs substrate		$p > 1\times10^{18}$ cm^{-3}	

Figure 1: Schematic of the superlattice GaAs photocathode with DBR structure. The GaAs surface layer was capped with amorphous As after the epitaxial growth.

SL-DBR photocathodes were grown in a MBE system at Sandia National Laboratories. Fig. 2 shows measured photoluminescence and reflectance of the SL-DBR and DBR layer. The SL-DBR structure photoluminescence peaks around 782 nm, and minimum reflectance is observed at around 781 nm. This is close to our design requirements, since 780 nm is typically the drive laser wavelength. The simulated DBR shows high reflectance and wide bandwidth $\Delta\lambda_B$.
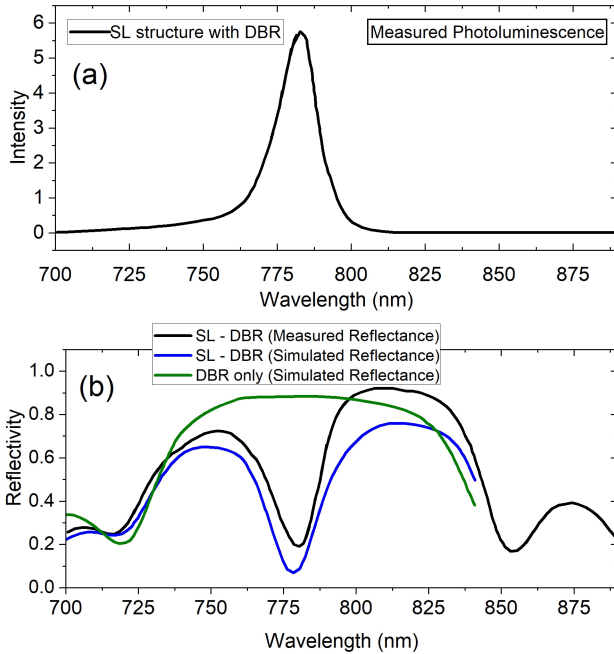
Figure 2: (a) Measured photoluminescence of SL structure with DBR, (b) measured and simulated reflectance of SL-DBR, and simulated reflectance of DBR.

We evaluated the crystal quality of the SL-DBR photocathode using transmission electron microscopy (TEM). TEM lamella was made using the in-situ lift-out method with a FEI Helios G5 UX DualBeam FIB/SEM with final Ga+ milling performed at 2 keV. TEM analysis was performed with a FEI Talos F200X TEM/STEM at an operating voltage of 200 keV with EDS data collected by 4 in-column integrated SSD Super-X detectors. Fig. 3 shows cross-sectional TEM/STEM images and EDS map of the SL-DBR photocathode. We did not observe any stacking faults or misfit dislocations [9] in the SL structure. Some threading dislocations are observed in the SL structure..
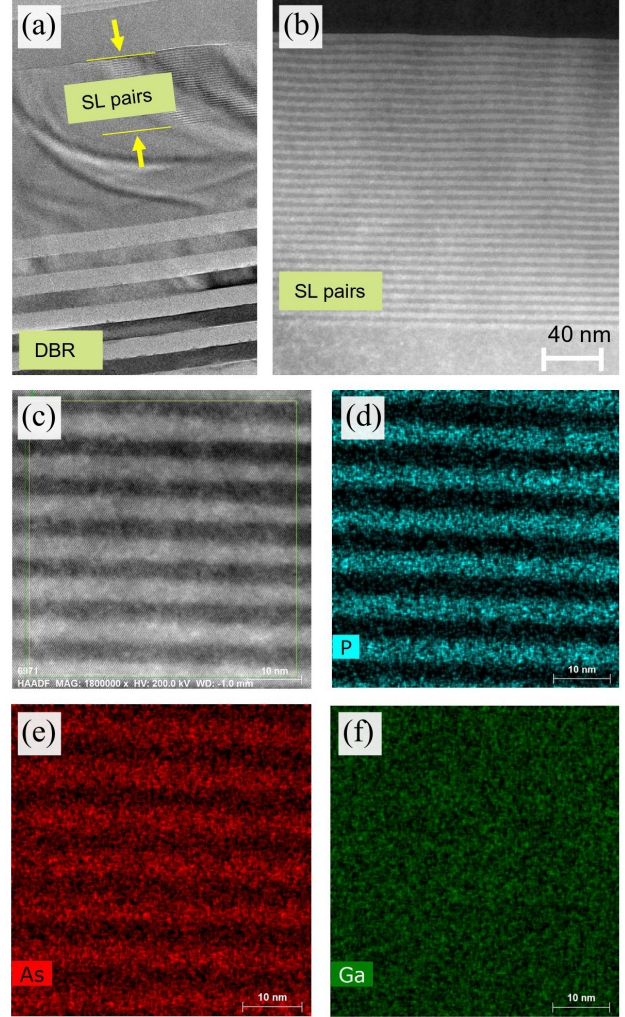
Figure 3: (a) Cross sectional TEM images of SL-DBR GaAs showing both SL and DBR pairs. Bend contours are visible which are associated with the bent sample with respect to the incident electron beam. The number of DBR-pairs was 10. (b) STEM image showing uniform SL-pairs (c) TEM image of a few SL-pairs, (d) EDS map of P, (e) EDS map of As, and (f) EDS map of Ga.

QE AND SPIN POLARIZATION

Photocathode samples were evaluated within a low-voltage retarding-field Mott polarimeter located at Brookhaven National Laboratory (BNL). A picture of this Mott polarimeter system is shown in Fig. 4. A new sample was attached to the cathode puck and loaded into the chamber through the load-lock manipulator that was

baked at 200°C for 72 hours. The sample was then heated to 500°C for 2 hours to remove the As cap and contamination from the surface under the vacuum pressure of 10^{-11} Torr scale. Then, the sample was activated at room temperature to form a negative electron affinity (NEA) surface using the standard yo-yo activation procedure with Cs and O_2. The QE of the sample was scanned with a laser with a wavelength ranging from 400 nm to 800 nm. A circularly polarized laser generated by a linear film polarizer and a quarter-wave plate finally illuminated the sample to obtain spin-polarized electrons, which were transferred into the spin detector through the spin deflector and transfer lens to measure the electron spin polarization (ESP).

Figure 4: The picture of the Mott polarimeter system at BNL, which is used for activation of photocathode and measurement of the QE and ESP.

The measured QE and ESP for the photocathode sample as a function of wavelength is shown in Fig. 5. This measurement is performed at the center of a 3-inch wafer. The peak QE obtained exceeds 15%, which is the highest ever reported photocathode QE at near-bandgap photon energies for SL-based photocathode. The maximum ESP found on this photocathode is around 70%. At the center of the wafer, both ESP and QE match the design requirements- both QE and ESP maximizes at around 780 nm. However, we have noticed that away from the center both peak QE and ESP deviate from the design requirement. A possible explanation for the non-uniformity across the 3" wafer may be related to a non uniform temperature across the wafer during the growth process leading to deviations from ideal composition and thickness. We are currently exploring different experimental conditions aimed at increasing the temperature uniformity to verify this hypothesis and meet design parameters over larger areas of the wafer. Fig. 6 shows QE and ESP with respect to wavelength measured away from the center on

the same wafer. The peak QE exceeds 10% and appears at around 760 nm wavelength. Peak ESP was around 75% and it maximize at around 780 nm. It is still lower than our target ESP of 85%, we are currently optimizing the SL-pair design to achieve higher ESP.
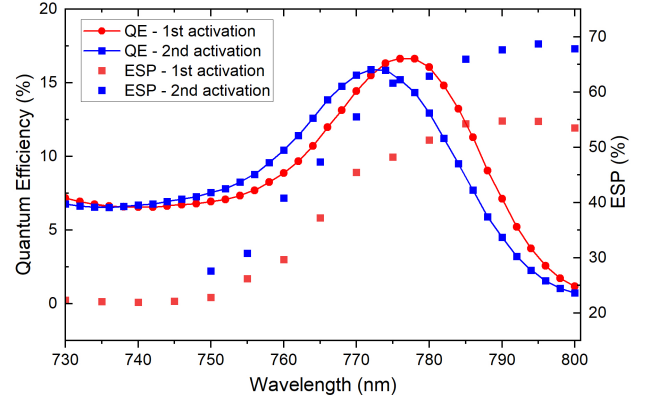

Figure 5: The QE and electron-spin polarization for the GaAs/GaAsP superlattice DBR photocathode as a function of the wavelength, measured at the center of the wafer.
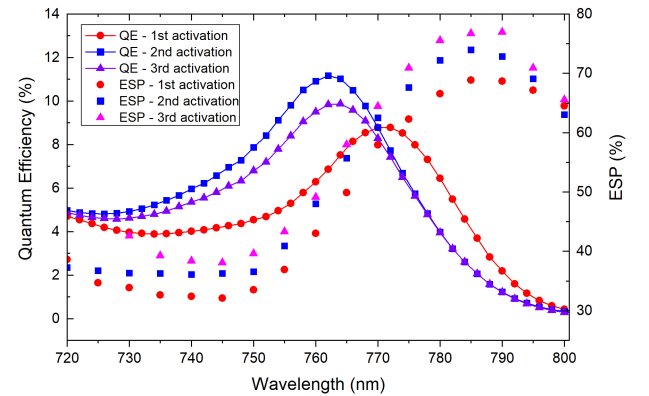

Figure 6: The QE and electron-spin polarization for the GaAs/GaAsP superlattice DBR photocathode as a function of the wavelength, measured at the edge of the wafer.

SUMMARY

In summary, we have fabricated superlattice GaAs/GaAsP based photocathodes with a DBR structure using molecular beam epitaxy. Photoluminescence and reflectance of the photocathode match with design requirements at around 780 nm wavelength. TEM analyses show minimum defects in the crystal, and SL and DBR structures are properly identified. With this type of photocathode, we obtained quantum efficiencies exceeding 15% and electron spin polarization of about 75% when illuminated with near bandgap photon energies. Further optimization is in progress to achieve even higher QE and electron spin polarization.

REFERENCES

[1] M. Kuwahara *et al.*, "30-kV spin-polarized transmission electron microscope with GaAs–GaAsP strained superlattice photocathode", *Appl. Phys. Lett.*, 101, 033102 (2012); https://doi.org/10.1063/1.4737177.

[2] C. Montag *et al.*, "Design Status update of the Electron Ion Collider", *12th Int. Particle Acc. Conf.*, IPAC2021, Campinas, SP, Brazil, 2021.

[3] E. Wang *et al.*, "High voltage dc gun for high intensity polarized electron source", *Phys. Rev. Accel. Beams.*, 25, 033401, 2022. https://doi.org/10.1103/PhysRevAccelBeams.25.033401

[4] T. Nakanishi *et al.*, "Large enhancement of spin polarization observed by photoelectrons from a strained GaAs layer", *Physics Letters A.*, Volume 158, Issues 6–7, 9 September 1991.

[5] X. Jin *et al.*, "Effect of crystal quality on performance of spin-polarized photocathode", *Appl. Phys. Lett.*, 105, 203509 (2014); https://doi.org/10.1063/1.4902337.

[6] W. Liu *et al.*, "Record-level quantum efficiency from a high polarization strained GaAs/GaAsP superlattice photocathode with distributed Bragg reflector", *Appl. Phys. Lett.*, 109, 252104 (2016); https://doi.org/10.1063/1.4972180.

[7] L. G. Gerchikov *et al.*, "Highly Effective Polarized Electron Sources Based on Strained Semiconductor Superlattice with Distributed Bragg Reflector", *AIP Conference Proceedings.*, 980, 124 (2008); https://doi.org/10.1063/1.2888077.

[8] T. Saka *et al.*, "New-Type Photocathode for Polarized Electron Source with Distributed Bragg Reflector", *Jpn. J. Appl. Phys.*, 32 L1837 (1993); https://iopscience.iop.org/article/10.1143/JJAP.32.L1837/pdf.

[9] X. Jin *et al.*, "Effects of defects and local thickness modulation on spin-polarization in photocathodes based on GaAs/GaAsP strained superlattices", *J. Appl. Phys.*, 108, 094509 (2010); https://doi.org/10.1063/1.3506658.